BABAR-PROC-03/65
SLAC-PUB-10190

Branching fractions and direct CP violation in B $\rightarrow$ PP(PV) decays

Marcella Bona
Università di Torino and INFN, Sezione di Torino
via Pietro Giuria 1
10125 Torino, Italy

I present the results of searches for B meson decays into two charmless mesons. I take into account final states made up of two pseudo-scalar (PP) or one pseudo-scalar and one vector (PV). The measurements use the data samples collected and analysed by the B-factory experiments at the $\Upsilon(4S)$ resonance energy: *BABAR*, Belle and CLEO.

1 Introduction

Charmless hadronic final states play an important role in the study of *CP*-violation. In the Standard Model, all *CP*-violating phenomena are a consequence of a single complex phase in the Cabibbo-Kobayashi-Maskawa (CKM) quark-mixing matrix [1].

Charmless decays of B mesons may proceed by $b \rightarrow u$, $b \rightarrow s$, or $b \rightarrow d$ transitions. The latter two mechanisms require flavor changing neutral currents which are not present at tree level in the Standard Model, and therefore must occur through suppressed processes such as the penguin mechanism. Such processes involve loops, which can get contributions from physics beyond the Standard Model. Even in the absence of such new physics, interference among competing amplitudes for a given decay mode can be exploited to measure CKM phases.

These charmless B decays in which CKM favored amplitudes are suppressed or forbidden are rare decays and they typically have branching fractions ($\mathcal{B}$) of less than 10^{-4}. Even if the branching fraction for these modes is expected to be so low, the present data samples available to *BABAR* and Belle Collaborations together with the new analysis effort by CLEO allow for measurements or stringent limits on many such modes.

In these years, the *BABAR* and Belle collaborations have reached solid results [2] on measurements of *CP*-violating asymmetries in B decays into final states containing charmonium, leading to strict constraints on the angle β of the CKM Unitarity Triangle.

In the Standard Model picture, the angle α can be related to time-dependent *CP*-violating asymmetries in the analysis of the decay $B^0 \rightarrow \pi^+\pi^-$ as well as in the case of three body $\pi^+\pi^-\pi^0$ decays in which such measurement would exploit interference between the $B^0 \rightarrow \rho^\pm\pi^\mp$ modes and the color-suppressed $B^0 \rightarrow \rho^0\pi^0$.

Ratios of branching fractions for various $\pi\pi$ and $K\pi$ decay modes are in principle sensitive to the angle γ [3], even if the measured branching fractions of all the $K\pi$ modes show a clear path which seems to suggest the dominance of the penguin amplitude over the others [4]. As a matter of fact the $K\pi$ modes (together with the relative PV modes like $K^*\pi$, ρK, ωK) are sensitive to γ through the Cabibbo-suppressed amplitude term which is proportional to $V_{ub}^* V_{us}$ but an interference between the latter and the Cabibbo-allowed amplitude term is needed in order to extract γ[1].

The extraction of α from measurements of the time-dependent asymmetry in $B^0 \to \pi^+\pi^-$ is complicated by the interference of tree and penguin amplitudes with different weak phases. The $B \to KK$ decays are characterized by similar penguin processes and, hence, can be used to isolate the tree and penguin contributions to $B^0 \to \pi^+\pi^-$. For example $K^0\overline{K}^0$ is a pure $b \to d$ penguin. The fact that no tree amplitude is possible, strongly reduces the expected branching fraction, but also allows to estimate the size of penguin contributions in $B \to \pi\pi$, once the $\mathcal{B}(B \to K^0\overline{K}^0)$ has been measured and SU(3) breaking effects have been taken into account. $K^\pm\overline{K}^0$ has the same penguin as $K^0\overline{K}^0$ plus an annihilation contribution. The comparison of the two branching fractions can be used to understand which is the real contribution coming from annihilation terms. Moreover, the entire $K^0\overline{K}^0$ amplitude is equal to the penguin contribution to the $\pi^0\pi^0$ channel, assuming SU(3). So, in the scenario of a large branching fraction for $\pi^0\pi^0$, the measurement of the $\mathcal{B}(K^0\overline{K}^0)$ can help to disentangle penguin contribution from other subleading terms in $\pi^0\pi^0$ amplitude. These other terms can be deduced in a similar way from K^+K^- decay which is a pure annihilation mode [5].

Also the decays of B-mesons to pseudo-scalar and vector particles provide opportunities for investigating the phenomenon of CP violation. Of particular interest are the quasi-two-body $B \to \rho\pi$ decays to three-pion final states. These can be used to measure the angles α and γ.

α can be determined from a full Dalitz plot analysis of the modes $B^0 \to \rho^\pm\pi^\mp$ and $B^0 \to \rho^0\pi^0$ [6]. The data sets available are still too small for this type of analysis. For the time being though, the *BABAR* experiment also performed a simultaneous measurement of branching fractions and CP-violating asymmetries in the decays $B^0 \to \rho^\pm\pi^\mp$ and $B^0 \to \rho^- K^+$ (and their charge conjugate) using a time-dependent maximum likelihood analysis. Following a quasi-two-body approach [7], the *BABAR* technique is restricting the analysis to the two regions of the $\pi^\mp\pi^0 h^\pm$ Dalitz plot ($h = \pi$ or K) that are dominated by either ρ^+h^- or ρ^-h^+. From this kind of analysis, the time-integrated and flavor-integrated charge asymmetries $A_{CP}^{\rho\pi}$ and $A_{CP}^{\rho K}$ that measure direct CP violation can be extracted together with the quantities $S_{\rho\pi}$ and $C_{\rho\pi}$ for the $\rho\pi$ mode.

Since, like in the two-body case, the extraction of α from $\rho^\pm\pi^\mp$ is complicated by the interference of decay amplitudes with different weak and strong phases, another strategy is to perform an SU(2) analysis using all $\rho\pi$ final states [9]. Assuming isospin symmetry, the angle α can be determined free of hadronic uncertainties from a pentagon relation formed in a complex plane by the five decay amplitudes $B^0 \to \rho^+\pi^-$, $B^0 \to \rho^-\pi^+$, $B^0 \to \rho^0\pi^0$, $B^+ \to \rho^+\pi^0$ and $B^+ \to \rho^0\pi^+$. These amplitudes can be determined from measurements of the corresponding decay rates and CP-asymmetries. γ can be extracted from the interference of $B^+ \to \chi_{c0}\pi^+$ and $B^+ \to \rho^0\pi^+$ in $B^+ \to \pi^+\pi^-\pi^+$ decays [8].

[1] For an example on this amplitude formalism see [5]

Also measurements of the charge asymmetries in the decay rates are reported according to the definition:

$$\mathcal{A}_{CP} = \frac{\Gamma\left(\overline{B} \to \overline{f}\right) - \Gamma\left(B \to f\right)}{\Gamma\left(\overline{B} \to \overline{f}\right) + \Gamma\left(B \to f\right)}.$$

Here and throughout this paper charge conjugate modes are implied. We also make use of the notation $h^{\pm}$ to represent a charged hadron that may be either a kaon or pion.

2 Analyses

The measurements presented in this paper are mainly based on the following data samples. The analyses of *BABAR* are based on $(87.9 \pm 1.0) \times 10^6$ $B\overline{B}$ pairs collected between 1999 and 2002 with the *BABAR* detector at the PEP-II asymmetric-energy B Factory at SLAC. This corresponds to an integrated luminosity of approximately $81\,\mathrm{fb}^{-1}$ at the $\Upsilon(4S)$ resonance. The results from Belle are based on $78\,\mathrm{fb}^{-1}$ data sample which corresponds to 85×10^6 $B\overline{B}$ pairs. The Belle detector[11] is a large-solid-angle general purpose spectrometer at the KEKB asymmetric-energy e^+e^- storage ring. The current CLEO data set is made up from the full CLEO II and CLEO III data samples totaling $15.3\,\mathrm{fb}^{-1}$. CLEO[12] is a general purpose solenoidal magnet detector operated at the Cornell Electron Storage Ring (CESR), a symmetric-energy storage ring tuned to provide center of mass energies near the $\Upsilon(4S)$ resonance.

Hadronic events are selected based on track multiplicity and event topology. Tracks are identified as pions or kaons using the various Particle Identification (PID) techniques described below. Candidate K^0_S mesons are reconstructed from pairs of oppositely charged tracks that form a well-measured vertex and have an invariant mass within a defined window around the nominal K^0_S mass [16]. The candidate must have a displaced vertex and flight direction consistent with a K^0_S originating from the interaction point. Candidate π^0 mesons are formed from pairs of photons with an invariant mass within a defined window around the nominal π^0 mass. The π^0 candidates are then kinematically fitted with their mass constrained to the nominal π^0 mass [16].

Reconstructed B candidates are identified using two kinematic variables: the beam-energy substituted mass (or beam-energy constrained mass) $m_{ES} = \sqrt{(E^{\mathrm{CM}}_{\mathrm{beam}})^2 - (p^{\mathrm{CM}}_B)^2}$ and the energy difference $\Delta E = E^{\mathrm{CM}}_B - E^{\mathrm{CM}}_{\mathrm{beam}}$, where $E^{\mathrm{CM}}_{\mathrm{beam}}$ is the beam energy, p^{CM}_B and E^{CM}_B are the momentum and the energy of the reconstructed B meson in the center-of-mass system (CM).

In these charmless modes, the largest source of background comes from random combinations of tracks and neutrals produced in the $e^+e^- \to q\overline{q}$ continuum (where $q = u$, d, s or c). These backgrounds are suppressed using the event topology. In the CM frame this background typically exhibits a two-jet structure that can produce two high momentum, nearly back-to-back particles, in contrast to the spherically symmetric nature of the low momentum $\Upsilon(4S) \to b\overline{b}$ events. This topology difference is exploited by making use of event-shape quantities. Various techniques and variables are used.

In the *BABAR* analyses, a preliminary requirement is applied on the angle θ_{sph} [15] between the sphericity axes, evaluated in the CM frame, of the B candidate and the remaining tracks

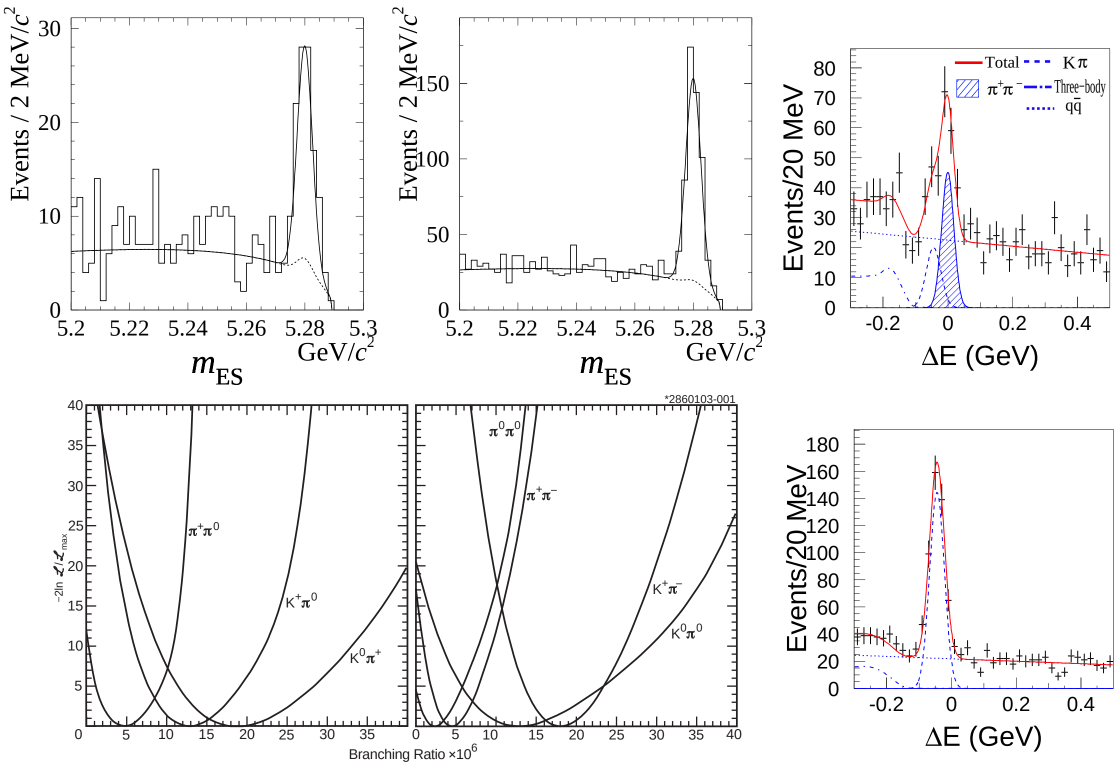

Figure 1: Examples of plots from the various two-body analyses and techniques. See text in Sect. 3 for details.

and photons in the event. The distribution of the absolute value of $\cos\theta_{sph}$ is strongly peaked near 1 for continuum events and is approximately uniform for $B\overline{B}$ events.

Another similarly powerful variable is the flight direction of the B candidate given by $\cos\theta_B = \hat{\mathbf{p}}\cdot\hat{\mathbf{z}}$ where $\mathbf{p}$ is the vector sum of the daughter momenta and $\mathbf{z}$ is the beam axis. Since the vector $\Upsilon(4S)$ is produced in e^+e^- annihilation it has a polarization $J_z = \pm 1$, and the subsequent flight direction of the pseudo-scalar B mesons is distributed as $|Y_1^{\pm 1}(\theta,\phi)|^2 \sim \sin^2\theta = 1-\cos^2\theta$. Background events are flat in this variable.

Another quantity largely used in the charmless analyses is a Fisher discriminant $\mathcal{F}$ which consists of an optimized linear combination of variables that distinguish signal from background [17].

BABAR analyses use a two-variable Fisher discriminant with $\sum_i p_i$ and $\sum_i p_i|\cos\theta_i|^2$ where p_i is the momentum and θ_i is the angle with respect to the thrust axis of the B candidate, both in the CM frame, for all tracks and neutral clusters not used to reconstruct the B meson.

Belle's technique consists of forming signal and background likelihood functions, $\mathcal{L}_S$ and $\mathcal{L}_{BG}$, from two variables. One is a Fisher discriminant determined from six modified Fox-Wolfram moments [14] and the other is $\cos\theta_B$. Requirements are imposed on the likelihood ratio $LR = \mathcal{L}_S/(\mathcal{L}_S + \mathcal{L}_{BG})$ for candidate events.

CLEO builds its Fisher discriminant as a linear combination of fourteen variables including the direction of the thrust axis of the candidate with respect to the beam axis, $\cos\theta_{thr}$, and

mode	BR (10^{-6}) [UL @ 90% CL]			
	CLEO	*BABAR*	Belle	WA
$B^0 \to \pi^+\pi^-$	$4.5^{+1.4+0.5}_{-1.2-0.4}$	$4.7 \pm 0.6 \pm 0.2$	$4.4 \pm 0.6 \pm 0.3$	4.6 ± 0.4
$B^0 \to K^+\pi^-$	$18.0^{+2.3+1.2}_{-2.1-0.9}$	$17.9 \pm 0.9 \pm 0.7$	$18.5 \pm 1.0 \pm 0.7$	18.2 ± 0.8
$B^0 \to K^+K^-$	< 0.8	< 0.6	< 0.7	< 0.6
$B^+ \to K^0\pi^+$	$18.8^{+3.7+2.1}_{-3.3-1.8}$	$22.3 \pm 1.7 \pm 1.1$	$22.0 \pm 1.9 \pm 1.1$	21.8 ± 1.4
$B^+ \to K^+\pi^0$	$12.9^{+2.4+1.2}_{-2.2-1.1}$	$12.8^{+1.2}_{-1.0} \pm 1.0$	$12.8 \pm 1.4^{+1.4}_{-1.0}$	12.8 ± 1.1
$B^0 \to K^0\pi^0$	$12.8^{+4.0+1.7}_{-3.3-1.4}$	$11.4 \pm 1.7 \pm 0.8$	$12.6 \pm 2.4 \pm 1.4$	11.9 ± 1.5
$B^+ \to K^0K^+$	< 3.3	< 2.5	< 3.4	< 2.5
$B^0 \to K^0\overline{K}^0$	< 3.3	< 1.8	< 3.2	< 1.8
$B^+ \to \pi^+\pi^0$	$4.6^{+1.8+0.6}_{-1.6-0.7}$	$5.5^{+1.0}_{-0.9} \pm 0.6$	$5.3 \pm 1.3 \pm 0.5$	5.3 ± 0.8
$B^0 \to \pi^0\pi^0$	< 4.4	< 3.6	< 4.4	< 3.6

Table 1: Branching Fraction results for PP charmless modes: $\pi\pi$, $K\pi$ and KK with all charge combinations [18]. Also the world averages are given.

the nine conical bins of a "Virtual Calorimeter". They are the scalar sum of the momenta of all tracks and photons (excluding the B candidate daughters) flowing into nine concentric cones centered on the thrust axis of the B candidate, in the CM frame. Each cone subtends an angle of $10°$ and is folded to combine the forward and backward intervals. In addition, the momentum of the highest momentum electron, muon, kaon, and proton are used as inputs to the Fisher discriminant taking advantage of the high quality particle identification in CLEO III.

In the case of a candidate mode involving one or more charged pions or kaons, such as $B \to K\pi$ or $B \to \pi\pi^0$, each charged track must be positively identified as K or π.

PID in *BABAR* analyses is accomplished with the Cherenkov angle measurement from a detector of internally reflected Cherenkov light (DIRC). The final fit to the data includes the normalized Cherenkov residuals $\left(\theta_c - \theta_c^\pi\right)/\sigma_{\theta_c}$ and $\left(\theta_c - \theta_c^K\right)/\sigma_{\theta_c}$, where θ_c is the measured Cherenkov angle of the charged primary daughter, σ_{θ_c} is its error, and θ_c^π (θ_c^K) is the expected value for a pion(kaon). The latter two quantities are measured separately for negatively and positively charged pions and kaons, from a sample of $D^0 \to K^-\pi^+$ originating from D^{*+} decays.

PID in Belle experiment is based on the light yield in the aerogel Cherenkov counter (ACC) and dE/dx measurements on the central drift chamber. For each hypothesis (K or π), the dE/dx and ACC probability density functions are combined to form likelihoods, $\mathcal{L}_K$ and $\mathcal{L}_\pi$. K or π mesons are distinguished by requirements on the likelihood ratio $\mathcal{L}_K/(\mathcal{L}_K + \mathcal{L}_\pi)$.

The K/π identification in CLEO relies on the pattern of Cherenkov photon hits in the RICH detector fitted to both a kaon and pion hypothesis, each with its own likelihood $\mathcal{L}_K$ and $\mathcal{L}_\pi$. Calibrated dE/dx information from the drift chamber is used to compute a χ^2 for kaon and pion hypotheses. The RICH and dE/dx results are combined to form an effective χ^2 difference, $\Delta_{K\pi} = -2\ln\mathcal{L}_K + 2\ln\mathcal{L}_\pi + \chi^2_K - \chi^2_\pi$. Kaons are identified by $\Delta_{K\pi} < \delta_K$ and pions by $-\Delta_{K\pi} < \delta_\pi$, with values of δ_K and δ_π chosen to yield $(90 \pm 3)\%$ efficiency as determined in an independent study of tagged kaons and pions obtained from the decay

mode	BR (10^{-6}) [UL @ 90% CL]			
	CLEO	*BABAR*	Belle	WA
$B^0 \to \rho^+\pi^-$	$27.6^{+8.4}_{-7.4} \pm 4.2$	$22.6 \pm 1.8 \pm 2.2$	$20.8^{+6.0+2.8}_{-6.3-3.1}$	22.7 ± 2.5
$B^+ \to \rho^0\pi^+$	$10.4^{+3.3}_{-3.4} \pm 2.1$	$24 \pm 8 \pm 3$	$8.0^{+2.3}_{-2.0} \pm 0.7$	9.5 ± 2.0
$B^+ \to \rho^+\pi^0$	< 43	–	–	< 43
$B^0 \to \rho^0\pi^0$	< 5.5	< 10.6	< 5.3	< 5.3
$B^0 \to \rho^+K^-$	$16^{+8}_{-6} \pm 3$	$7.3^{+1.3}_{-1.2} \pm 1.2$	< 23	7.7 ± 1.7
$B^+ \to \rho^0K^+$	< 17	< 29	< 12	< 12
$B^+ \to \rho^+K^0$	< 48	–	–	< 48
$B^0 \to \rho^0K^0$	< 39	–	< 12	< 12

Table 2: Branching Fraction results from the ρh modes with h being a π or a K with all charge combinations.

$D^{*+} \to \pi^+ D^0$ ($D^0 \to K^-\pi^+$).

Finally PV modes allow for the use of the vector particle helicity angle θ_h defined as the angle between the direction of one of h daughters in the h rest frame and the direction of h in the B rest frame.

3 Results

In general the charmless decay modes taken into account here have contributions from (a) signal, (b) continuum $q\overline{q}$ background and (c) cross-feed from other B modes.

In order to extract the signal yields, *BABAR* and CLEO use unbinned extended maximum likelihood fit. The input variables to the fit are in general m_{ES}, ΔE, Fisher discriminant $\mathcal{F}$. Some *BABAR* analyses take advantage of a Neural Network to fight the continuum background instead of the Fisher discriminant. In CLEO analyses, the flight direction of the B candidate $\cos\theta_B$ is added to the fit inputs. Moreover most of the charmless decay analyses in *BABAR* include also the Cherenkov angle in the fit to distinguish when necessary among differences in the K/π content of the final states.

In Belle analyses, the signal yields are extracted by a binned maximum likelihood fit to the ΔE distribution in the m_{ES} signal window (5.271 GeV/c^2 $< m_{ES} <$ 5.289 GeV/c^2, the lower limit being 5.270 GeV/c^2 in case of a π^0 in the final state). The m_{ES} distributions are fitted as a consistency check.

Tables 1, 2 and 3 show the Branching Fraction results of respectively the charmless two-body hadronic B decays [18], the modes with a ρ in the final states [19], the modes with a K^*, a ϕ or an ω in the final states [20]. The results shown are from all the three experiments and also the relative world averages are reported.

In Figure 1 plots are shown from the various two-body analyses and techniques. The top right left are two examples from *BABAR* analyses and represent the projections of the m_{ES} distributions from the unbinned maximum likelihood fit for events that satisfy optimized requirements on probability ratios for signal to background based on all variables except m_{ES}

mode	BR (10^{-6}) [UL @ 90% CL]			
	CLEO	*BABAR*	Belle	WA
$B^+ \to K^{*0}\pi^+$	$7.6^{+3.5}_{-3.0} \pm 1.6$	$15.5 \pm 3.4 \pm 1.8$	$19.4^{+4.2+4.1}_{-3.9-7.1}$	12.3 ± 2.6
$B^+ \to K^{*+}\pi^0$	< 31	$-$	$-$	< 31
$B^0 \to K^{*+}\pi^-$	$16^{+6}_{-5} \pm 2$	$-$	< 30	16 ± 6
$B^0 \to K^{*0}\pi^0$	< 3.6	$-$	< 7	< 3.6
$B^+ \to \phi K^+$	$5.5^{+2.1}_{-1.8} \pm 0.6$	$10.0^{+0.9}_{-0.8} \pm 0.5$	$9.4 \pm 1.1 \pm 0.7$	9.3 ± 0.8
$B^0 \to \phi K^0$	$5.4^{+3.7}-2.7 \pm 0.7$	$7.6^{+1.3}_{-1.2} \pm 0.5$	$9.0 \pm 2.2 \pm 0.7$	7.7 ± 1.1
$B^0 \to \phi K^{*0}$	$11.5^{+4.5+1.8}_{-3.7-1.7}$	$11.1^{+1.3}_{-1.2} \pm 0.8$	$10.0^{+1.6+0.7}_{-1.5-0.8}$	10.7 ± 1.1
$B^+ \to \phi K^{*+}$	$10.6^{+6.4+1.8}_{-4.9-1.6}$	$12.1^{+2.1}_{-1.9} \pm 1.1$	$6.7^{+2.1+0.7}_{-1.9-1.0}$	9.4 ± 1.6
$B^+ \to \omega K^+$	$3.2^{+2.4}_{-1.9} \pm 0.8$	$5.0 \pm 1.0 \pm 0.4$	$6.7^{+1.3}_{-1.2} \pm 0.6$	5.4 ± 0.8
$B^+ \to \omega\pi^+$	$1.3^{+3.3}_{-2.9} \pm 1.4$	$5.4 \pm 1.0 \pm 0.5$	$5.9^{+1.4}_{-1.3} \pm 0.6$	5.3 ± 0.9
$B^0 \to \omega K^0$	$10.0^{+5.4}_{-4.2} \pm 1.4$	$5.3^{+1.4}_{-1.2} \pm 0.5$	< 7.6	5.6 ± 1.4

Table 3: Branching Fraction results for PV final states including K^*, ϕ or ω.

itself. The bottom left plots show the distributions of $-2\ln(\mathcal{L}/\mathcal{L}_{\max})$ for CLEO II and CLEO III combined for the $K\pi$ and $\pi\pi$ modes with non-zero yields. The remaining right plots are two examples from Belle and show the ΔE distributions in the m_{ES} signal region for $\pi^+\pi^-$ and $K^+\pi^-$ respectively. The results of the fits used to extract the signal yields are also shown.

In Table 4 the asymmetry results are shown from all three collaborations. All the results are compatible with zero and still statistical dominated.

The additional statistics that will be collected in the next years by *BABAR* and Belle will provide exciting results in the physics of charmless decay.

mode	CLEO	*BABAR*	Belle	WA
$B^0 \to K^+\pi^-$	$-0.04 \pm 0.16 \pm 0.02$	$-0.10 \pm 0.04 \pm 0.01$	$-0.07 \pm 0.06 \pm 0.01$	-0.09 ± 0.03
$B^+ \to K^+\pi^0$	$-0.29 \pm 0.23 \pm 0.02$	$-0.09 \pm 0.09 \pm 0.01$	$0.23 \pm 0.11^{+0.01}_{-0.04}$	0.00 ± 0.07
$B^0 \to K^0\pi^+$	$0.18 \pm 0.24 \pm 0.02$	$-0.05 \pm 0.08 \pm 0.01$	$0.07^{+0.09+0.01}_{-0.08-0.03}$	0.01 ± 0.06
$B^+ \to K^0\pi^0$	$-$	$0.03 \pm 0.36 \pm 0.09$	$-$	0.03 ± 0.37
$B^+ \to \pi^+\pi^-$	$-$	$0.30 \pm 0.25 \pm 0.04$	$0.77 \pm 0.27 \pm 0.08$	0.51 ± 0.19
$B^+ \to \pi^+\pi^0$	$-$	$-0.03^{+0.18}_{-0.17} \pm 0.02$	$-0.14 \pm 0.24^{+0.05}_{-0.04}$	-0.07 ± 0.15
$B^+ \to \rho^-\pi^+$	$-$	$-0.11^{+0.16}_{-0.17} \pm 0.04$	$-$	-0.11 ± 0.17
$B^+ \to \rho^+\pi^-$	$-$	$-0.62^{+0.24}_{-0.28} \pm 0.06$	$-$	-0.62 ± 0.29
$B^+ \to K^+\rho^-$	$-$	$0.28 \pm 0.17 \pm 0.08$	$-$	0.28 ± 0.19

Table 4: Direct *CP* asymmetry results for $K\pi$, $\pi\pi$, $\rho\pi$ and ρK modes

References

[1] N. Cabbibo, Phys. Rev. Lett. **10**, 531 (1963); M. Kobayashi and T. Maskawa, Prog. Theor. Phys. **49**, 652 (1973).

[2] *BABAR* Collaboration, B. Aubert *et al.*, Phys. Rev. Lett. **89**, 201802 (2002); Belle Collaboration, K. Abe *et al.*, Phys. Rev. D **66**, 071102 (2002).

[3] M. Beneke, G. Buchalla, M. Neubert and C. T. Sachrajda, Nucl. Phys. B **606** 245 (2001); Y. Y. Keum, H. N. Li and A. I. Sanda, Phys. Rev. D **63** 054008 (2001).

[4] M. Ciuchini *et al.*, Phys. Lett. B **515** 33 (2001).

[5] A. J. Buras and L. Silvestrini, Nucl. Phys. B **569**, 3 (2000).

[6] A.E. Snyder and H.R. Quinn, Phys. Rev. D **48**, 2139 (1993).

[7] *BABAR* Collaboration, "The *BABAR* Physics Book", (P. Harrison and H. Quinn eds.), SLAC-R-504 (1998).

[8] I. Bediaga *et al.*, Phys. Rev. Lett. **81**, 4067 (1998).

[9] H.J. Lipkin, Y. Nir, H.R. Quinn and A. Snyder, Phys. Rev. D **44**, 1454 (1991).

[10] *BABAR* Collaboration, B. Aubert *et al.*, Nucl. Instrum. and Methods A **479**, 1 (2002).

[11] Belle Collaboration, A. Abashian *et al.*, Nucl. Instr. and Meth. A **479**, 117 (2002).

[12] CLEO Collaboration, (CLEO II), CLNS-94-1277; D. Peterson *et al.*, Nucl. Instr. and Meth. **478**, 142 (2002); Y. Kubota *et al.*, (CLEO Collaboration), (CLEO III), Nucl. Instr. and Meth. A **320**, 66 (1992); T.S. Hill, Nucl. Instr. and Meth. A **418**, 32 (1998).

[13] G. C. Fox and S. Wolfram, Phys. Rev. Lett. **41**, 1581 (1978).

[14] Belle Collaboration, K. Abe *et al.*, hep-ex/0207090 (2002).

[15] S. L. Wu, Phys. Rep. C **107**, 59 (1984).

[16] Particle Data Group, Phys. Rev. D **66**, 010001 (2002).

[17] R.A. Fisher, *The Use of Multiple Measurements in Taxonomic Problems*, Annals of Eugenics, 7, (1936) 179; CLEO Collaboration, D.M. Asner *et al.*, Phys. Rev. D **53**, 1039 (1996).

[18] CLEO Collaboration, A. Bornheim *et al.*, Phys. Rev. D **68**, 052002 (2003); *BABAR* Collaboration, B. Aubert *et al.*, Phys. Rev. Lett. **91**, 021801 (2003), *BABAR* Collaboration, B. Aubert *et al.*, Phys. Rev. Lett. **89**, 281802 (2002); (for Belle Collaboration) T. Tomura, arXiv:hep-ex/0305036.

[19] CLEO Collaboration, C. P. Jessop *et al.*, Phys. Rev. Lett. **85**, 2881 (2000); Belle Collaboration, A. Gordon *et al.*, Phys. Lett. B **542**, 183 (2002).

[20] Heavy Flavor Averaging Group for rare decays for Winter 2003 Conferences, `http://www.slac.stanford.edu/xorg/hfag/rare/`.